

Collision Data and Population Modelling for W^{44+} : Dirac R -matrix and Non Close-coupling Electron Impact Calculations

Matthew M. Bluteau

ADAS Team, University of Strathclyde/CCFE/JET

2 October 2015

INAF — Osservatorio Astrofisico di Catania



Introduction

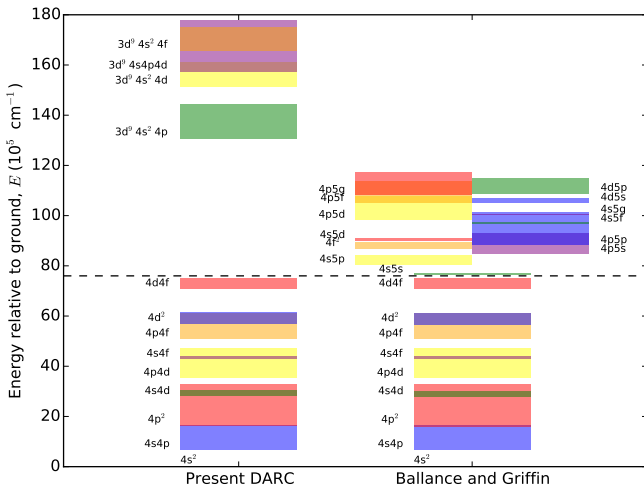
- Elemental tungsten (W) the primary material candidate for divertors in future fusion devices [1, 2, 3, 4, 5].
- The effects of this high Z (74), efficiently radiating, impurity species in the fusion plasma must be investigated.
- Quantitative estimates of emission line power losses due to W ions requires high quality, fundamental atomic data and their application in atomic population modeling; must be done on a per ion basis for complex cases.
- We present such work for W^{44+} [6], which has been identified in the core of JET (peak abundance $T_e \sim 3$ keV) with emission in the soft x-ray region due primarily to the transition arrays, $[3d^{10}4s^2-3d^94s^24f]$ and $[3d^{10}4s^2-3d^94s4p4d]$.
- With $Z = 74$, a relativistic technique should be used to generate the fundamental data: Dirac R -matrix calculations conducted via the DARC/GRASP⁰ suite.
- Comparison to previous DARC calculation by Ballance and Griffin [7]: critical $3d^94s^24f$ and $3d^{10}4s4p4d$ configurations were omitted.
- $P_{LT,1}$, $\mathcal{P}\mathcal{E}\mathcal{C}$, and $\mathcal{F}\text{-}\mathcal{P}\mathcal{E}\mathcal{C}$ derived data generated by our CR modeling.

Methodology

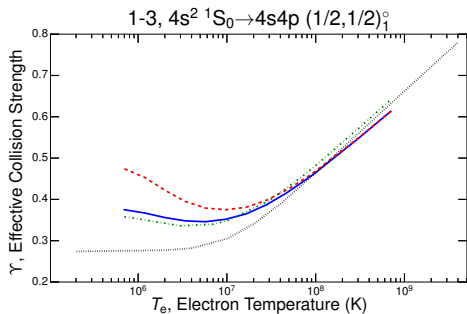
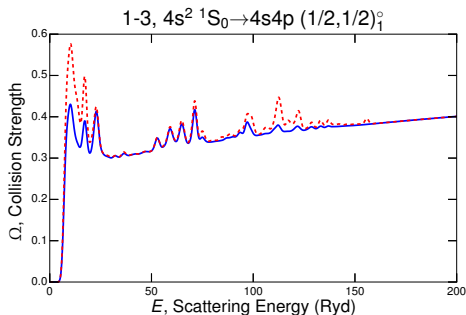
DARC/GRASP⁰ Key Parameters:

- Configuration interaction (CI) and close-coupling (CC) expansion:
 $[1s^2 2s^2 2p^6 3s^2 3p^6] 3d^{10} 4s^2, 3d^{10} 4s 4p, 3d^{10} 4s 4d, 3d^{10} 4s 4f, 3d^{10} 4p^2, 3d^{10} 4p 4d,$
 $3d^{10} 4p 4f, 3d^{10} 4d^2, 3d^{10} 4d 4f, 3d^9 4s^2 4p, 3d^9 4s^2 4d, 3d^9 4s^2 4f, 3d^9 4s 4p 4d$
- 313 $jjJ\pi$ levels total
- Type-I damping only: radiative transition of core, non-Rydberg electron from intermediate resonance; Ballance and Griffin include all forms
- Full CC equations solved for $0.5 \leq J \leq 16.5$; nonexchange for $17.5 \leq J \leq 35.5$
- R -matrix boundary = 1.33 au; maximum scattering energy = 1 100 Ryd; 34/30 basis orbitals per continuum angular momentum for exchange/nonexchange
- 48 000 energy mesh points in resonance region for asymptotic, outer region code
- AUTOSTRUCTURE Breit-Pauli distorted wave (BPDW) calculation conducted in conjunction

Atomic Structure: Configuration Energy Ranges

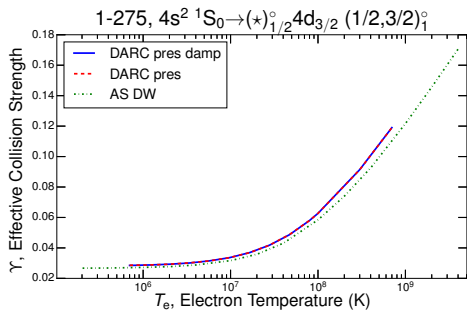
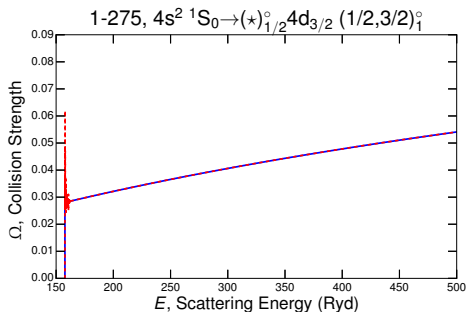


Collision Data 1: Low Transition Example



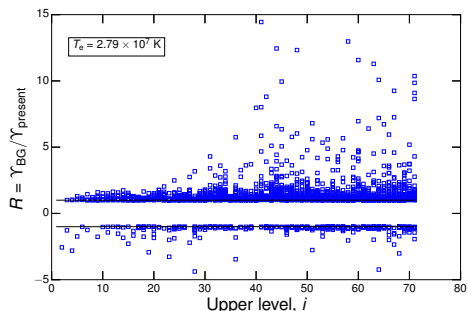
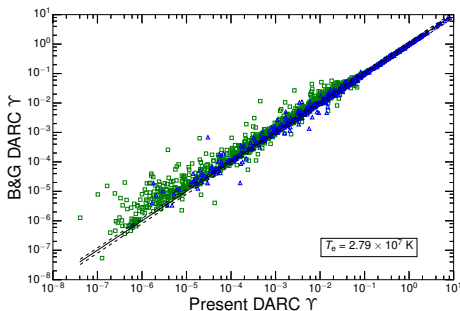
Collision strength, Ω , and effective collision strength, Υ , results for a low lying transition. The left figure is the convolution of the present Ω data with a 2.205 Ryd (30 eV) Gaussian function. The dashed (red) line is for the undamped data, and the solid (blue) line for the damped data. The right figure displays the present Υ data (dashed red and solid blue) along with the present AUTOSTRUCTURE DW (hashed black) results and the corresponding Ballance and Griffin (dash-dot green) results [7].

Collision Data 2: Soft X-ray Transition Example



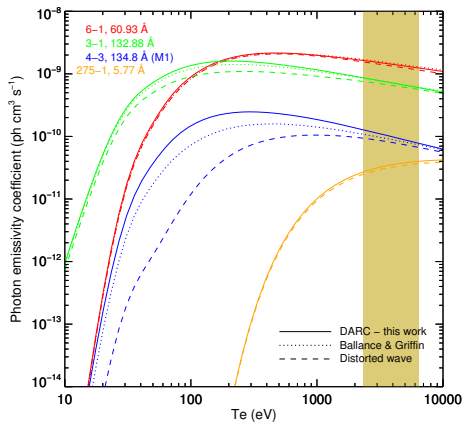
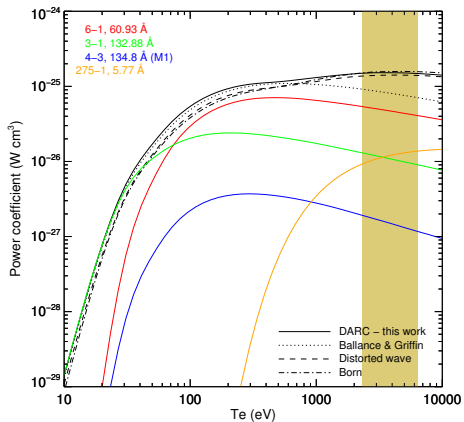
Example of a dominant 3d-subshell transition from the transition arrays, $[3d^{10}4s^2-3d^94s^24f]$ and $[3d^{10}4s^2-3d^94s4p4d]$. The left figure is the 'raw' Ω data sets that have not been convoluted. Again, the dashed (red) line is for the undamped data, and the solid (blue) line for the damped data. The right figure displays the Υ data for both the DARC and AUTOSTRUCTURE DW calculations. $\star \equiv (3d^9(^2D_{5/2})4s_{1/2})_2^{\circ}4p_{3/2}$.

Collision Data Comparison



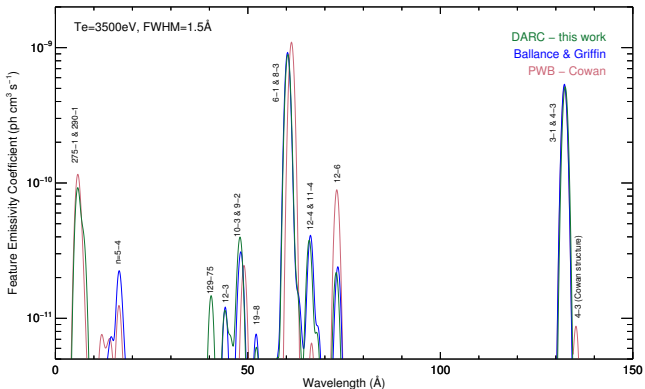
Comparison (left) and ratio (right) scatter plots of Υ values from Ballance and Griffin's (B&G) fully damped DARC versus the present, partially damped DARC. Comparison plot: the dotted lines demarcate the 20% error region around the $y = x$ line, and the percentage of points within the error region is: total = 63%, dipole = 82%, non-dipole = 56%. Ratio plot: the binary positive or negative behaviour of the ratio is defined by $R = \Upsilon_{\text{BG}}/\Upsilon_{\text{present}}$ if $\Upsilon_{\text{BG}} > \Upsilon_{\text{present}}$ or $R = -\Upsilon_{\text{present}}/\Upsilon_{\text{BG}}$ if $\Upsilon_{\text{BG}} < \Upsilon_{\text{present}}$. The ratio is plotted versus the upper level, i , of the transition in each case.

$P_{LT,1}$, $P_{L,1,j \rightarrow k}$, and $\mathcal{P}\mathcal{E}\mathcal{C}$ Derived Data



The shaded vertical bar represents the T_e range where the fractional abundance of W^{44+} in the coronal equilibrium approximation is greater than 0.1. Left: the total excitation line power coefficients, $P_{LT,1}$, as the enveloping (black) lines for all datasets, along with a selection of contributing $P_{L,1,j \rightarrow k}$ values from the present work. A sample of the strongest and most relevant contributing individual lines from the present DARC work have been emphasized (coloured) and labelled. Right: the corresponding $\mathcal{P}\mathcal{E}\mathcal{C}$ lines.

$\mathcal{F}\text{-}\mathcal{P}\mathcal{E}\mathcal{C}$ Derived Data



The envelope feature photon-emissivity coefficient, $\mathcal{F}\text{-}\mathcal{P}\mathcal{E}\mathcal{C}$, vectors for various W^{44+} calculations plotted versus wavelength at $T_e = T_i = 3.5$ keV. The Doppler broadening by the velocity distribution of the radiating ions has been applied using the default Maxwellian distribution with $T_i = T_e$. The results were also convolved with an ideal spectrometer instrument function with a FWHM of 1.5 Å. The vertical labelling of the peaks denotes the transition(s) for the dominant excitation $\mathcal{P}\mathcal{E}\mathcal{C}(s)$ within the feature

- Primacy of appropriate CI/CC expansion
- Appropriateness of non-CC approaches for power coefficients and radiated loss
- CC results needed for detailed spectroscopy
- Neglect of $n = 5$ configurations does not seem to impact modelled results greatly

References I

- [1] H. Bolt, V. Barabash, W. Krauss, J. Linke, R. Neu, S. Suzuki, and N. Yoshida. Materials for the plasma-facing components of fusion reactors. *J. Nucl. Mater.*, 329-333:66–73, August 2004.
- [2] G. Federici, C. H. Skinner, and J. N. Brooks. Plasma-material interactions in current tokamaks and their implications for next step fusion reactors. *Nucl. Fusion*, 41(12):1967, 2001.
- [3] R. A. Pitts, S. Carpentier, F. Escourbiac, T. Hirai, V. Komarov, S. Lisgo, A. S. Kukushkin, A. Loarte, M. Merola, A. Sashala Naik, R. Mitteau, M. Sugihara, B. Bazylev, and P. C. Stangeby. A full tungsten divertor for ITER: Physics issues and design status. *J. Nucl. Mater.*, 438:S48–S56, July 2013.
- [4] R. Aymar. Summary of the ITER final design report, ITER doc. G A0 FDR. Technical report, ITER, 2001.
- [5] R. Aymar, P. Barabaschi, and Y. Shimomura. The iter design. *Plasma Phys. Control. Fusion*, 44(5):519–565, 2002.
- [6] M. M. Bluteau, M. G. O’Mullane, and N. R. Badnell. Dirac R -matrix and Breit-Pauli distorted wave calculations of the electron-impact excitation of W^{44+} . *J. Phys. B*, 48(195701):18, 2015.
- [7] C. P. Ballance and D. C. Griffin. Electron-impact excitation of w^{44+} and w^{45+} . *J. Phys. B*, 40(2):247–258, 2007.